

Numerical Simulation of $\text{Cu}_2\text{ZnSnS}_4$ Based Solar Cells with In_2S_3 Buffer Layers by SCAPS-1D

Peijie Lin[†], Lingyan Lin[†], Jinling Yu*, Shuying Cheng, Peimin Lu and Qiao Zheng

Institute of Micro/Nano Devices and Solar Cells, School of Physics & Information Engineering, Fuzhou University, Fuzhou 350108, P.R. China

Abstract

The performance of the $\text{Cu}_2\text{ZnSnS}_4$ based solar cell is investigated using a simulation program called Solar Cell Capacitance Simulator (SCAPS). The cell structure is based on $\text{Cu}_2\text{ZnSnS}_4$ (CZTS) compound semiconductor as the absorber layer, *n*-doped and un-doped (*i*) zinc oxide as the window layer, In_2S_3 as the buffer layer. We study the influence of the defect density, carrier density, thickness of the CZTS absorber layer, working temperature, In_2S_3 buffer layer thickness and its carrier density on the cell performance. The simulation results illustrate that the optimal layer thickness is from 2500 to 3000 nm for the absorber layer, and that in the range of 20 to 30 nm for the buffer layer. Besides, controlling the CZTS defect density under $1 \times 10^{13} \text{ cm}^{-3}$ is very necessary for high efficiency CZTS cells. The increased working temperature has a strong influence on the solar cell efficiency and the temperature coefficient is calculated to be about $-0.17\%/K$. An optimal photovoltaic property has been achieved with an efficiency of 19.28% (with $J_{sc} = 23.37 \text{ mA/cm}^2$, $V_{oc} = 0.958 \text{ V}$ and $FF = 86.13\%$). All these simulation results will give some important guides for feasibly fabricating higher efficiency CZTS solar cells.

Key Words: CZTS, In_2S_3 , SCAPS, Solar Cells

1. Introduction

Over recent years, a good amount of efforts have been made to study the $\text{Cu}_2\text{ZnSnS}_4$ based thin-film solar cells [1–7]. $\text{Cu}_2\text{ZnSnS}_4$ is a quaternary semiconductor with excellent photovoltaic properties such as high absorption coefficient over 10^4 cm^{-1} , and a direct band gap value about 1.4–1.5 eV, which is very close to the optimum band gap value of the single-junction solar cells. Moreover all the chemical elements in CZTS are non-toxic and abundant. In comparison with other thin film solar cells, CZTS based solar cells are gradually becoming excellent low-cost alternatives [8]. They have been fabricated using many kinds of techniques, such as elec-

troplating [4], thermal evaporation [5], and co-sputtering [6]. At present, the best CZTS solar cell has been obtained using the structure of Al/ZnO:Al/ZnO/CdS/CZTS/Mo/SLG with an efficiency of 8.4% [7], (11.1% [9] with the Se-containing $\text{Cu}_2\text{ZnSn}(\text{S},\text{Se})_4$). However, the CdS buffer layer can cause serious pollution and absorption loss due to its low band gap. It is necessary to substitute the CdS buffer layer for other nontoxic and wider band gap materials. Among them In_2S_3 is one of the most promising candidate materials because of its stability and higher band gap in comparison with CdS [10,11]. V. G. Rajeshmon et al. have reported an efficiency of 1.85% on the CZTS cell with In_2S_3 buffer layer [12]. However, when compared with some other solar cells (e.g. CIGS based solar cells), which have been studied extensively [13], the understanding of the CZTS/ In_2S_3 heterojunction solar cells is relatively limited. In order to improve the CZTS cell efficiency and fully understand the perfor-

*Corresponding author. E-mail: jlyu@semi.ac.cn

[†]Peijie Lin and Lingyan Lin contributed equally to this study and should be considered co-first authors.

mance of cells, it is necessary to systematically investigate the influence of the basic factors in the performance of the cells.

Numerical simulation is an efficient way to predict the effect of changes in material properties, assess the potential merits of cell structures and then optimize the structure of cells. At present, there is lack of numerical simulation report about the CZTS/In₂S₃ heterojunction solar cells. Therefore, in this work, a numerical simulation based on SCAPS is performed to investigate the effect of CZTS layer defect density, carrier density, thickness, In₂S₃ thickness and operating temperature on the cell performance. Finally, the optimized parameters for the CZTS/In₂S₃ heterojunction solar cells with an efficiency of 19.28% have been obtained in our numerical simulation.

2. Methodologies

SCAPS-1D is an one-dimensional solar cell simulation software that developed at the Department of Electronics and Information Systems of Gent University, Belgium [14]. It is generally developed for polycrystalline thin-film devices. In comparison with other simulation softwares, SCAPS has the largest number of AC and DC electrical measurements including short circuit current density (J_{sc}), fill factor (FF), open circuit voltage (V_{oc}), conversion efficiency (Eff), quantum efficiency (QE), spectral response, generation and recombination profile, which is based on the hole and electron continuity equations together with Poisson equation. All these physical quantities can be calculated in light and dark

condition and also at different illuminations and temperatures. The good agreements between the experimental results and the SCAPS simulation results motivate us to use the simulation tool in this work [15–17].

The cell structure used in our simulation is n -ZnO:Al/ i -ZnO/ n -In₂S₃/ p -CZTS, as shown in Figure 1. This cell structure consists of two window layers, namely, a highly conductive n -type Al-doped ZnO (n -ZnO) and an intrinsic ZnO layer (i -ZnO). The baseline values of the physical parameters used in the study are all cited from experimental study, reasonable estimates in some cases [5,8,18], or literatures, which are summarized in Table 1. In the simulation we didn't take the influence of the shunt resistance and series resistance into consideration. In each material layer only one type of the single level defects is introduced in order to make the simulation model as simple as possible. These defects are all compensating defects that positioned at the intrinsic level which is close to the midgap. The default operating tem-

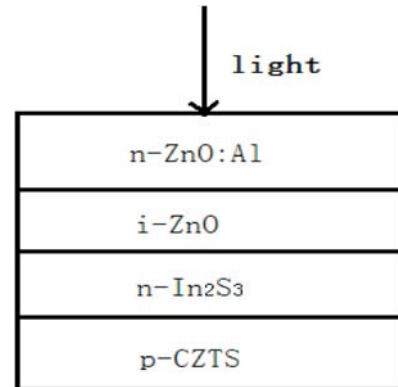


Figure 1. Structure of CZTS solar cell used in the numerical simulation.

Table 1. Physical parameters used in the simulation

Parameters	p -CZTS	n -In ₂ S ₃	i -ZnO	n -ZnO:Al
Thickness, W (nm)	2500	50	50	200
Relative permittivity	10	13.5	9	9
Electron affinity (eV)	4.5	4.7	4.6	4.6
E_g (eV)	1.5	2.8	3.3	3.3
N_c (cm ⁻³)	2.2×10^{18}	1.8×10^{19}	2.2×10^{18}	2.2×10^{18}
N_v (cm ⁻³)	1.8×10^{19}	4×10^{13}	1.8×10^{19}	1.8×10^{19}
Electron mobility (cm ² ·V ⁻¹ ·s ⁻¹)	100	400	100	100
Hole mobility (cm ² ·V ⁻¹ ·s ⁻¹)	25	210	25	25
Donor concentration (cm ⁻³)	0	1×10^{17}	1×10^5	1×10^{18}
Acceptor concentration (cm ⁻³)	1×10^{17}	10	0	0
Gaussian defect density (cm ⁻³)	1×10^{12}	1×10^{18}	1×10^{18}	1×10^{18}

perature is set to 300 K and the illumination condition is set to the global AM.1.5 standard.

3. Results and Discussion

3.1 Effect of CZTS Absorber Thickness

At the start of the simulation, the thickness of the CZTS layer is changed from 500 nm to 4000 nm to study the influence of absorber layer thickness in the cell performance, while other material parameters of different layers are kept unchanged. The cell performance and QE output with varied CZTS absorber layer thickness are shown in Figures 2 and 3, respectively. It can be found from Figure 2 that both the J_{sc} and V_{oc} of the solar cell are increased with the increasing thickness of CZTS layer. This is mainly because that the thicker absorber layer will absorb more photons with longer wavelength, which will in turn make a contribution to the generation of electron-hole pairs. However, almost a linear decrease of J_{sc} can be found when the CZTS layer thickness is less than 1000 nm, which can be mainly attributed to the incomplete absorption of the incident photons and increasing recombination of photo-generated carriers at the back contact, which is located near the depletion region in a cell with thin absorber layer. Thus, less photo-generated

electrons can contribute to the quantum efficiency. We can find out that the solar cell efficiency increases with the CZTS absorber layer thickness, but it has a much slower increasing rate when the layer thickness is over 2500 nm, so does the increasing trend of the quantum efficiency, which means that the thickness of 2500 nm is enough to absorb most of the incident photons. Therefore, if one takes the processing times and material usage into account, fabricating the CZTS solar cells with thick absorber layer will not be very cost effective. So in the

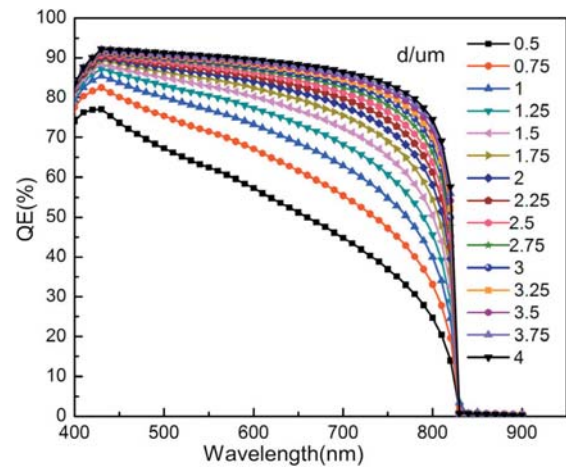


Figure 3. Effect of absorbing layer thickness on spectral response of the cells.

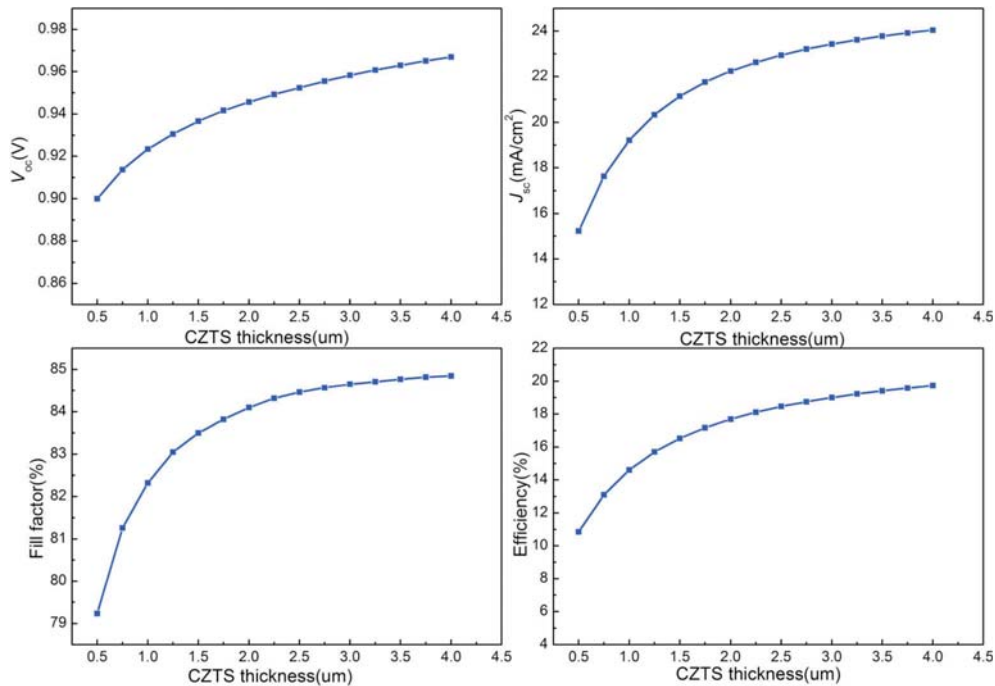


Figure 2. The dependence of cell performance on the CZTS layer thickness.

later numerical simulation, we adopt the CZTS layer thickness to be 2500 nm.

3.2 Effect of Absorber Carrier Density

The influence of carrier densities (N_A) in the CZTS absorbing layer on the J - V characteristics of the cells is illustrated in Figure 4. It shows that the J_{sc} decreases with increasing absorber doping while V_{oc} increases with it. The PN junction model can help us explain this phenomenon, which is described by the following equation:

$$I_0 = Aqn_i^2 \left(\frac{D_e}{L_e N_A} + \frac{D_h}{L_h N_D} \right), V_{oc} = \frac{kT}{q} \ln \left(\frac{I_L}{I_0} + 1 \right) \quad (1)$$

Here A is the quality factor of the diode, I_0 is the saturation current, n_i is the intrinsic concentration, q is the electronic charge, I_L is the light-generated current, T is the temperature, k is Boltzmann's constant, L is the diffusion length, D is the diffusion coefficient, N_D and N_A are the donor and acceptor doping concentrations respectively. The subscripts h and e refer to holes and electrons, respectively. When the absorber carrier densities N_A are increased, the saturation current I_0 will be reduced, and then resulting in the increase of the V_{oc} . However, the short-circuit current will decrease with the increasing of carrier densities. This is mainly due to the fact that the higher carrier densities will enhance the recombination process and reduce the probability of the collection of photon-generated electron, and the quantum efficiency of the long wavelength photons will also be reduced. The photons of long wavelength will be absorbed deeply in the CZTS layer, therefore, the collected efficiency of the electrons created there are more dependent on the diffusion effect. In CZTS films, The resistivity and carrier densities are dependent on the ratio of Cu/(Zn+Sn). The Cu-rich and Zn-poor films have extremely high carrier densities and low resistivity, which are not suitable for fabricating solar cells. Higher efficiency cells can be obtained using Zn-rich, Cu-poor CZTS absorber layers [3].

3.3 Effect of CZTS Layer Defect Density

In the CZTS solar cells, the defect states can introduce additional carrier recombination centers, they can enhance the recombination process of photo-generated carriers, thus leading to the increase of reverse saturation

current density, the reduction of open-circuit voltage, cell efficiency and short-circuit current. To quantitatively analyze the influence of defect states on solar cell performance, we introduce Gaussian defect states in the CZTS layer. The defect level is positioned at the middle of the band gap, the value ranges from $1 \times 10^9 \text{ cm}^{-3}$ to $1 \times 10^{17} \text{ cm}^{-3}$. Figure 5 illustrates the dependence of the photovoltaic properties of the cell on the defect densities in the CZTS layer. It can be found that when the CZTS defect density is less than $1 \times 10^{13} \text{ cm}^{-3}$ the overall cell performance remains nearly unchanged. However, when the defect density in the CZTS layer is above $1 \times 10^{13} \text{ cm}^{-3}$, all the output parameters of the cell are affected strongly, and they decrease dramatically with the increase of the defect density. When the defect density reaches $1 \times 10^{17} \text{ cm}^{-3}$, the conversion efficiency is only 3%. The simulation results indicate that, in order to improve the photovoltaic characteristics of solar cells, controlling the defect density under $1 \times 10^{13} \text{ cm}^{-3}$ by improving the process conditions is very necessary.

3.4 Effect of the Thickness and Carrier Densities (N_D) in the In_2S_3 Buffer Layer

In our simulation, the influence of In_2S_3 thickness on solar cell performance is also investigated. The thickness of In_2S_3 layer is changed from 1 to 140 nm, and simulation results are illustrated in Figure 6. It can be seen that, although the increase of buffer layer thickness decreases J_{sc} , V_{oc} , FF and Eff , the reduction is not so significant for FF and V_{oc} as that for J_{sc} and Eff . This phenomenon can

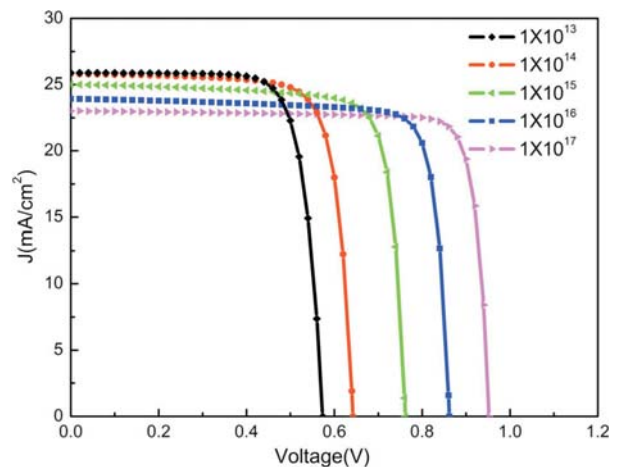


Figure 4. J - V of cells with different carrier densities in the CZTS absorber.

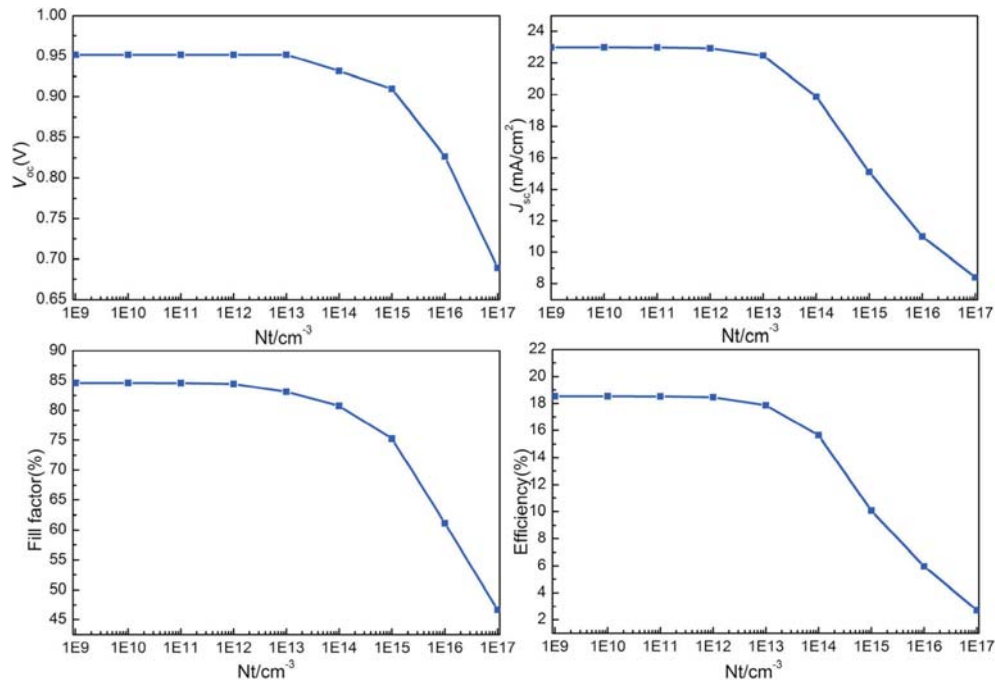


Figure 5. Cell performances with different defect density in the CZTS layer.

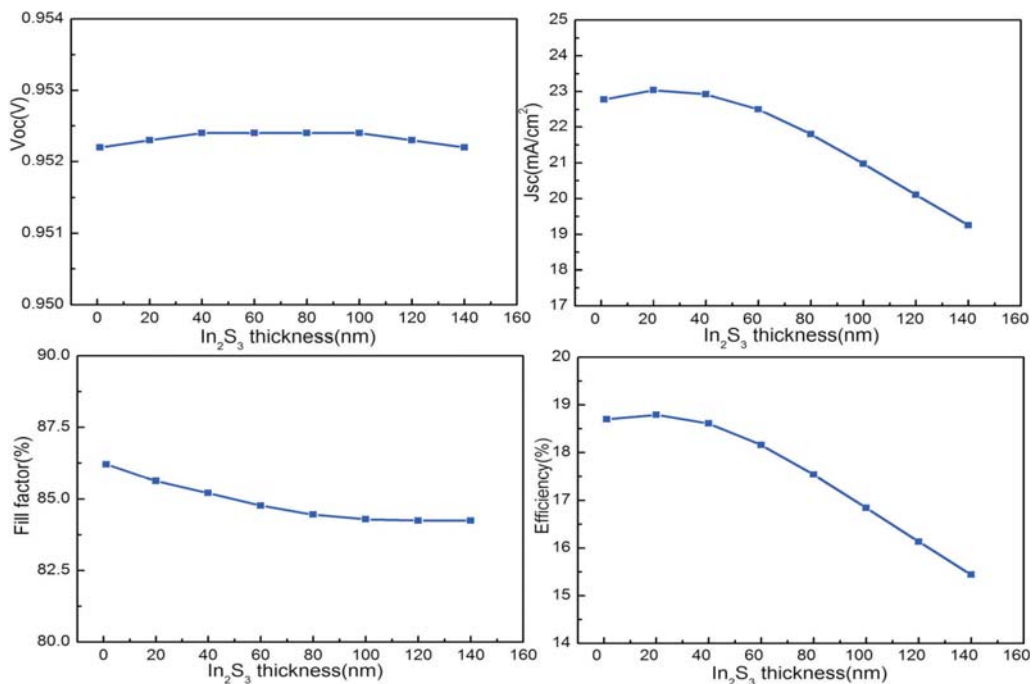


Figure 6. Cell performance with various In_2S_3 layer thicknesses.

be attributed to the photon loss that happens on a thick buffer layer. That is, as the buffer layer thickness is increased, more incident photons will be absorbed by the In_2S_3 layer, which will result in a decrease of photons that can be captured by the absorber layer. Therefore, the

absorbed photons will produce less electron-hole pairs, thus decreasing the quantum efficiency of the cell, as illustrated in Figure 7. With increasing In_2S_3 thickness, a drastic drop in the J_{sc} and Eff is observed for thicker films. And the reason that the thinner buffer layer shows

higher performance comes from a minimum thickness of the strained buffer layer appears to be needed to compensate the effect of misfit dislocation due to lattice mismatch between the In_2S_3 and CZTS. However, for very thin buffer layer (< 10 nm) a reduction of V_{oc} , J_{sc} and E_{ff} is found. Too thin buffer layer may result into leakage current and too thick one could lead to low carrier separation rate. From the above, the optimized and the preferred buffer layer thickness is in the range from 20 nm to 30 nm for CZTS solar cell in the simulation. Figure 8 illustrates the dependence of the cell efficiency on the thickness of the buffer layer with different carrier densities. The carrier densities (N_D) is varied from 1×10^{17} cm^{-3} to 1×10^{19} cm^{-3} . It shows that the conversion efficiency decreases with the increasing of the carrier density, due to the reduction of the width of the space charge region and the decrease of the collection efficiency of the photo-generated carriers which are induced by a higher carrier density in the buffer layer.

3.5 Optimization of the $n\text{-ZnO:Al}/i\text{-ZnO}/n\text{-In}_2\text{S}_3/p\text{-CZTS}$ Solar Cell

According to the simulation results shown above, in the range of parameters selected, the optimal photovoltaic properties with an efficiency of 19.28% (with $J_{sc} = 23.37$ mA/cm^2 , $V_{oc} = 0.958$ V and $FF = 86.13\%$) can be achieved when the thickness and carrier densities of the CZTS is 3000 nm and 1×10^{17} cm^{-3} , respectively, the

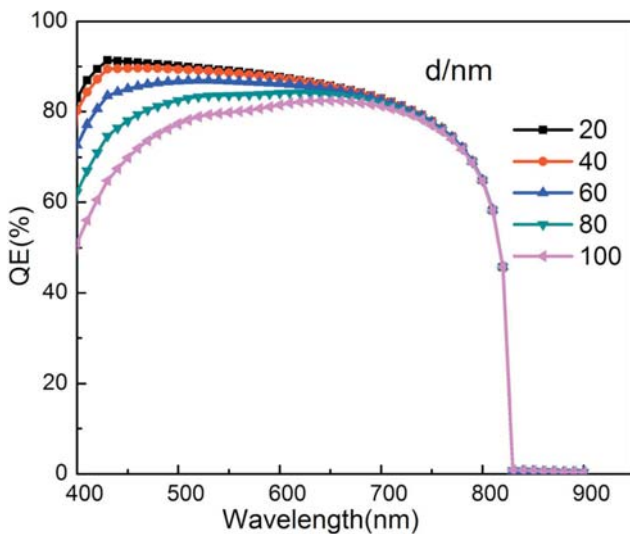


Figure 7. Effect of buffer layer thickness on spectral response of the cells.

CZTS defect density is 1×10^{12} cm^{-3} and the carrier densities and the thickness of the In_2S_3 are 1×10^{17} cm^{-3} and 20 nm, respectively. And other structure parameters are kept unchanged as shown in Table 1.

3.6 Effects of Working Temperature on CZTS Solar Cells

Working temperature plays a significant part in the performance of solar cells. The solar cell panels are usually installed in the outdoor. Sunlight will cause the heating of the solar panels, thus increasing the working temperature. So the solar cells often operate at a temperature which is higher than 300 K. The influences of the working temperature on the CZTS cell performance have been investigated using working temperature changed from 300 K to 450 K. The simulation results in Figure 9 illustrate that the overall cell performance is decreasing with the increase of the working temperature. Parameters such as band gaps of the materials, the carrier concentration, hole and electron mobility would be affected at a higher temperature, and finally results in a lower cell efficiency [7]. And the temperature coefficient of the conversion efficiency is found to be about $-0.17\%/K$. V_{oc} decreases with the increased temperature because of the temperature dependence on the reverse saturation current. The reverse saturation current is increasing with the increased temperature, and the increase in the saturation current decreases the open circuit voltage. The electrons in the solar cells will gain additional energy when the

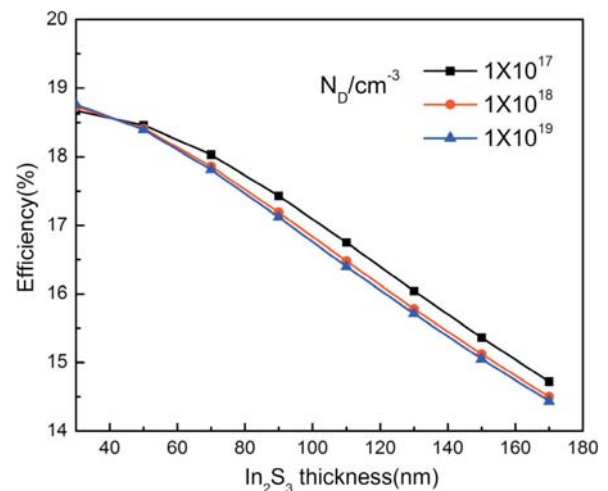


Figure 8. Efficiency of cells with different carrier densities in the In_2S_3 buffer layer.

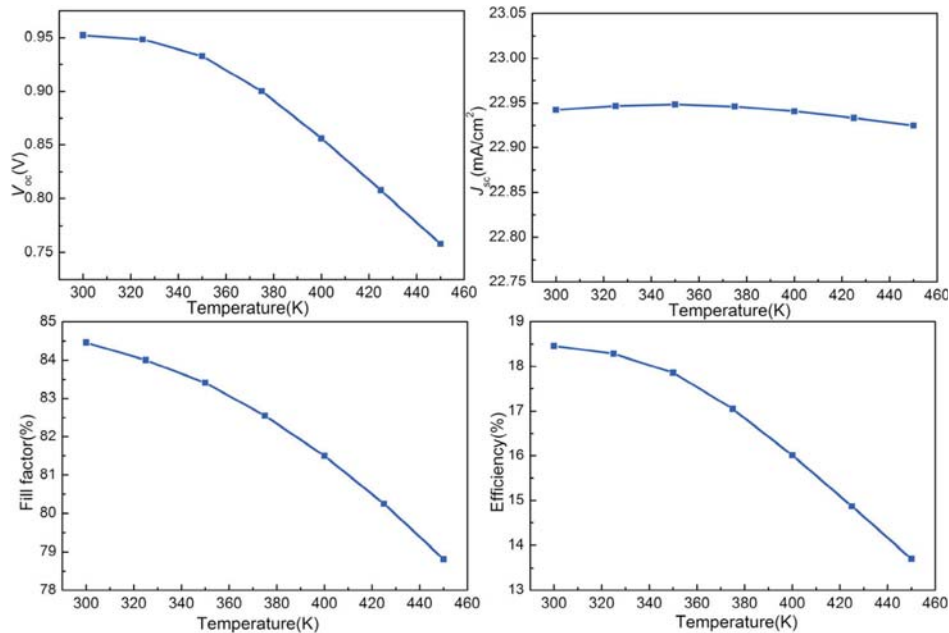


Figure 9. The dependence of cell performance on the operation temperature.

operating temperature is increased. So they will become unstable at higher temperature and are more likely to be recombined with the holes before they could reach the depletion region and be collected.

4. Conclusions

In conclusion, the CZTS/ In_2S_3 heterojunction solar cell performance is numerically simulated by using SCAPS-1D package. The numerical simulations have been done by adjusting parameters such as the defect density, carrier density, thickness of the CZTS absorber layer, working temperature, In_2S_3 buffer layer thickness and its carrier density to analyze their effects on the cell performance. The simulations show that the optimized thickness for the absorbing layer and the buffer layer should be from 2500 to 3000 nm and 20 to 30 nm, respectively. Besides, controlling the defect density under $1 \times 10^{13} \text{ cm}^{-3}$ is very necessary for excellent photovoltaic characteristics of the solar cells, which can be realized by improving the process conditions. In the range of calculation, the optimal photovoltaic properties has been achieved with an efficiency of 19.28% (with $FF = 86.13\%$, $V_{oc} = 0.958 \text{ V}$ and $J_{sc} = 23.37 \text{ mA/cm}^2$) when the thickness and carrier density of the CZTS is 3000 nm and $1 \times 10^{17} \text{ cm}^{-3}$, respectively, the CZTS defect density is 1

$\times 10^{12} \text{ cm}^{-3}$ and the thickness and the carrier density of the In_2S_3 is 20 nm and $1 \times 10^{17} \text{ cm}^{-3}$, respectively. The temperature coefficient of conversion efficiency is calculated to be about $-0.17\%/K$. The results above will give some important guide for feasibly fabricating higher efficiency CZTS solar cells.

Acknowledgements

This work was supported by the National Nature Sciences Funding of China (61076063, 61306120) and Fujian Provincial Department of Science & Technology, China (2012J01266).

References

- [1] Moholkar, A. V., Shinde, S. S., Babar, A. R., et al., "Development of CZTS Thin Films Solar Cells by Pulsed Laser Deposition: Influence of Pulse Repetition Rate," *Solar Energy*, Vol. 85, No. 7, pp. 1354–1363 (2011). doi: 10.1016/j.solener.2011.03.017
- [2] Moritake, N., Fukui, Y., Oonuki, M., et al., "Preparation of $\text{Cu}_2\text{ZnSnS}_4$ Thin Film Solar Cells under Non-Vacuum Condition," *Phys. Status Solidi C*, Vol. 6, No. 5, pp. 1233–1236 (2009). doi: 10.1002/pssc.200881158

- [3] Katagiri, H., Jimbo, K., Yamada, S., et al., "Enhanced Conversion Efficiencies of $\text{Cu}_2\text{ZnSnS}_4$ -Based Thin Film Solar Cells by Using Preferential Etching Technique," *Appl. Phys. Exp.*, Vol. 1, pp. 041201–041202 (2008). doi: [10.1143/APEX.1.041201](https://doi.org/10.1143/APEX.1.041201)
- [4] Ennaoui, A., Lux-Steiner, M., Weber, A., et al., " $\text{Cu}_2\text{ZnSnS}_4$ Thin Film Solar Cells from Electroplated Precursors: Novel Low-Cost Perspective," *Thin Solid Films*, Vol. 517, No. 7, pp. 2511–2514 (2009). doi: [10.1016/j.tsf.2008.11.061](https://doi.org/10.1016/j.tsf.2008.11.061)
- [5] Wang, K., Gunawan, O., Todorov, T., et al., "Thermally Evaporated $\text{Cu}_2\text{ZnSnS}_4$ Solar Cell," *Appl. Phys. Lett.*, Vol. 97, p. 143508 (2010). doi: [10.1063/1.3499284](https://doi.org/10.1063/1.3499284)
- [6] Katagiri, H., Jimbo, K., Maw, W. S., et al., "Development of CZTS-Based Thin Film Solar Cells," *Thin Solid Films*, Vol. 517, No. 7, pp. 2455–2460 (2009). doi: [10.1016/j.tsf.2008.11.002](https://doi.org/10.1016/j.tsf.2008.11.002)
- [7] Shin, B., Gunawan, O., Zhu, Y., et al., "Thin Film Solar Cell with 8.4% Power Conversion Efficiency Using an Earth-Abundant $\text{Cu}_2\text{ZnSnS}_4$ Absorber," *Prog. Photovolt: Res. Appl.*, Vol. 21, No. 1, pp. 72–76 (2013). doi: [10.1002/pip.1174](https://doi.org/10.1002/pip.1174)
- [8] Seol, J. S., Lee, S. Y., Lee, J. C., et al., "Electrical and Optical Properties of $\text{Cu}_2\text{ZnSnS}_4$ Thin Films Prepared by RF Magnetron Sputtering Process," *Sol. Energy Mater. Sol. Cells*, Vol. 75, No. 1–2, pp. 155–162 (2003). doi: [10.1016/S0927-0248\(02\)00127-7](https://doi.org/10.1016/S0927-0248(02)00127-7)
- [9] Todorov, T. K., Tang, J., Bag, S., et al., "Beyond 11% Efficiency: Characteristics of State-of-the-Art $\text{Cu}_2\text{ZnSn}(\text{S},\text{Se})_4$ Solar Cells," *Adv. Energy Mater.*, Vol. 3, No. 1, pp. 34–38 (2012). doi: [10.1002/aenm.201200348](https://doi.org/10.1002/aenm.201200348)
- [10] Pistor, P., Caballero, R., Hariskos, D., et al., "Quality and Stability of Compound Indium Sulphide as Source Material for Buffer Layers in $\text{Cu}(\text{In},\text{Ga})\text{Se}_2$ Solar Cells," *Sol. Energy Mater. Sol. Cells*, Vol. 93, No. 1, pp. 148–152 (2009). doi: [10.1016/j.solmat.2008.09.015](https://doi.org/10.1016/j.solmat.2008.09.015)
- [11] Benchouk, K., Ouerfelli, J., Saadoun, M., et al., "Optical and Electrical Characterization of In_2S_3 Buffer Layer for Photovoltaics Applications," *Physics Procedia*, Vol. 2, No. 3, pp. 971–974 (2009). doi: [10.1016/j.phpro.2009.11.051](https://doi.org/10.1016/j.phpro.2009.11.051)
- [12] Rajeshmon, V. G., Poornima, N., Sudha, K. C., et al., "Modification of the Optoelectronic Properties of Sprayed In_2S_3 Thin Films by Indium Diffusion for Application as Buffer Layer in CZTS Based Solar Cell," *J. Alloys Comp.*, Vol. 553, pp. 239–244 (2013). doi: [10.1016/j.jallcom.2012.11.106](https://doi.org/10.1016/j.jallcom.2012.11.106)
- [13] Repins, I., Contreras, M. A., Egaas, B., et al. "19.9%-Efficient $\text{ZnO}/\text{CdS}/\text{CuInGaSe}_2$ Solar Cell with 81.2% Fill Factor," *Prog. Photovolt: Res. Appl.*, Vol. 16, No. 3, pp. 235–239 (2008). doi: [10.1002/pip.822](https://doi.org/10.1002/pip.822)
- [14] Burgelman, M., Nollet, P. and Degraeve, S., "Modeling Polycrystalline Semiconductor Solar Cells," *Thin Solid Films*, Vol. 361–362, pp. 527–532 (2000). doi: [10.1016/S0040-6090\(99\)00825-1](https://doi.org/10.1016/S0040-6090(99)00825-1)
- [15] Marlein, J., Decock, K. and Burgelman, M., "Analysis of Electrical Properties of CIGSSe and Cd-Free CIGSSe Solar Cells," *Thin Solid Films*, Vol. 517, No. 7, pp. 2353–2356 (2009). doi: [10.1016/j.tsf.2008.11.048](https://doi.org/10.1016/j.tsf.2008.11.048)
- [16] Nollet, P., Burgelman, M. and Degraeve, S., "The Back Contact Influence on Characteristics of CdTe/CdS Solar Cells," *Thin Solid Films*, Vol. 361–362, pp. 293–297 (2000). doi: [10.1016/S0040-6090\(99\)00760-9](https://doi.org/10.1016/S0040-6090(99)00760-9)
- [17] Khelia, S., Verschraegen, J., Burgelman, M., et al., "Numerical Simulation of the Impurity Photovoltaic Effect in Silicon Solar Cells," *Renewable Energy*, Vol. 33, No. 2, pp. 293–298 (2008). doi: [10.1016/j.renene.2007.05.027](https://doi.org/10.1016/j.renene.2007.05.027)
- [18] Hossain, M. I., Vanathan, P. C., Zaman, M., et al., "Prospect of Indium Sulphide as an Alternative to Cadmium Sulphide Buffer Layer in CIS Based Solar Cells from Numerical Analysis," *Chalcogenide Letters*, Vol. 8, No. 5, pp. 315–324 (2011).

Manuscript Received: May 5, 2014

Accepted: Aug. 1, 2014